

Machine learning study of single-atom platinum supported on graphene nanostructures (SAC Pt-G)

Beatriz Andrea C. Tan, Yuji Hamamoto, Yoshitada Morikawa
Osaka University Graduate School of Engineering

1. Introduction

Platinum (Pt) supported on graphene is an established catalyst for CO oxidation, oxygen reduction, and other fuel cell reactions, but the cost and rarity of platinum necessitates further research into reducing Pt loading. The single-atom catalyst configuration stabilized on a support, namely, graphene, maximizes catalyst surface area and minimizes catalyst loading, but faces issues related to low reactivity and instability due to sintering or poisoning [1–3]. Single atom catalyst Pt on graphene (SAC Pt-G) has been successfully synthesized through various methods, and SAC Pt-G synthesized through atomic layer deposition has exhibited a reduced overpotential and resistance to catalyst deactivation compared to commercially available Pt-C [4,5].

SAC Pt-G favors edge adsorption, as Pt terminates dangling C bonds in vacancies and edges, based on the observed experimental structures and overlapping local density of states (LDOS) [6]. DFT studies by Wella et al. employed density functional theory (DFT) to determine Pt-SAC adsorption sites and stability on zigzag and graphene nanoribbons, also confirming the preferential edge adsorption of Pt, as opposed to vacancy substitution within the graphene plane [7]. Adsorption studies also show enhanced performance compared to pure Pt(111) [8].

However, single atoms tend to cluster or sinter in situ and Pt-SAC is difficult to stabilize, thus, we aim to identify viable structures for synthesis and factors that enhance the stability of these structures. While DFT-based computational approaches can accurately model the structural properties and adsorption behavior of SAC-Pt G, this is executed at great

computational cost. To speed up the individual energy and force calculations in structural optimization, machine learning (ML) techniques can be implemented to reduce the number of first-principles (FP) calculations.

In particular, we use the GOFEE algorithm, or Global Optimization with First-principles Energy Expression [9,10] to identify stable and metastable structures of SAC Pt-G on the hydrogenated graphene edge of nanoflake graphene, armchair graphene nanoribbon (AGNR), and zigzag graphene nanoribbon (ZGNR) structures.

Additionally, we also investigate the effect of nitrogen doping on the stability and reactivity of SAC Pt-G and its reactivity. Experimental studies have shown that N adsorbed adjacent to SAC Pt increases the stability of Pt by increasing the population of the Pt $5d_{yz}$ orbital, allowing for stronger Pt-C binding [11]. However, a more detailed analysis, assessing several possible atomic arrangements, is required to determine the dominant structures of N-doped SAC Pt-G and their behaviors in adsorption studies.

2. Computational Details

2.1. The GOFEE algorithm

To determine the structure with the lowest energy, known as the global minimum, GOFEE uses a combination of Gaussian process regression and FP calculations to train a surrogate model on the fly, rather than using a predetermined training database. The surrogate model speeds up the relaxation steps by using Gaussian process regression to relax new candidate structures instead of FP calculations. This is performed by executing several steps, where each step

consists of 1) mutating the population, 2) relaxing the system via a surrogate model, producing the surrogate energy (E_{sur}), 3) selecting the best candidate using $f(x)$, 4) evaluating the candidate using FP, then 5) training the surrogate model to improve the accuracy of the structure search towards finding the GM. This training data is used to update the population and surrogate model. The acquisition function $f(x)$ in Step 3 depends on minimizing the surrogate energy while encouraging exploration, determined by the parameter κ and the uncertainty σ_{sur} .

$$f(x) = E_{sur}(x) - \kappa\sigma_{sur}(x) \quad \text{Eq. 1}$$

The candidate with the minimum $f(x)$ is evaluated in Step 4 using two single-point FP calculations, one of which is slightly perturbed to calculate atomic forces.

For this study, 30 independent runs of 300 steps were performed, employing the Generalized Projector Augmented Wave (GPAW) method [12,13] to evaluate the total energy using the Linear Combination of Atomic Orbitals (LCAO) method with a Perdew-Burke-Erzerhof (PBE) atomic setup [14,15]

The ability of the structure search to identify the global minimum is quantified by the success curve, which is the fraction of independent runs that have identified the global minimum structure and energy as a function of the number of FP calculations. Candidates with a final success rate of at least 15% are selected from the search, then evaluated for stability and reactivity using DFT.

2.2. Structure search

To evaluate graphene nanoribbon systems using GOFEE, armchair and zigzag nanoribbon starting scaffolds with monohydrogenated bottom edges were prepared according to Figure 1, and free C, H, N, and Pt atoms were allowed to move freely within the boundary indicated. For the armchair and zigzag nanoribbon structure searches, the set of free atoms contain combinations of 5-8 C atoms, 0-8 H atoms,

and 1 Pt atom. However, the experimental graphene edge is more closely approximated by a flake graphene model containing both armchair and zigzag edges, as opposed to a nanoribbon. The starting scaffold approximates half of a coronene molecule ($C_{10}H_6$) fixed in place, with additional 10-14 C, 5-8 H, and 1 Pt atoms allowed to move freely within the boundary indicated in Figure 1. In all cases, the effect of N doping was also investigated by adding 1-2 N atoms to the set of free atoms.

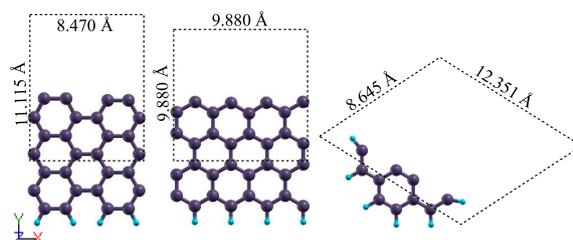


Figure 1. Scaffolds used in the SAC Pt-G structure search with boundaries outlined.

2.3. Structure Evaluation

Selected candidates produced by the structure search were evaluated using FP DFT calculations to assess their stability and reactivity, indicated by the binding energy of Pt and the adsorption energy of reaction intermediates. Candidates with the lowest energy within 0.2 eV of the GM and a success rate of at least 15% were further optimized using DFT to accurately assess the stability. Geometric optimization was performed, employing ultrasoft pseudopotentials and rev-vdW-DF2 corrections in the Quantum Espresso 7.2 software package [16,17].

3. Results

A comparison of sample ZGNR, AGNR, and flake structures alongside their success rates is presented in Figure 2 and Figure 3. The structure search easily identifies the GM at low degrees of freedom, but is still successful at identifying the GM even with many free C atoms. However, increasing H tends to decrease the success rate of the search on the same scaffold.

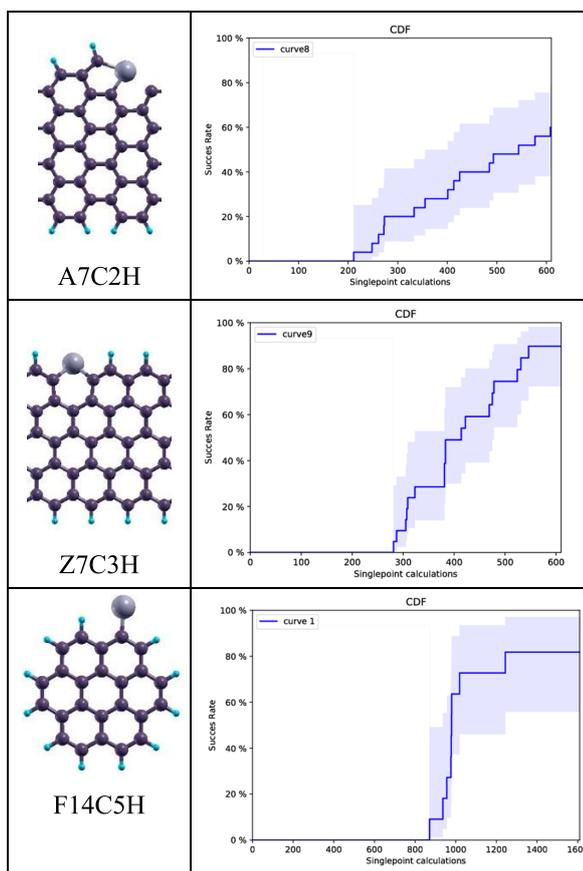


Figure 2. Global minimum and success rates of selected SAC Pt-G structures.

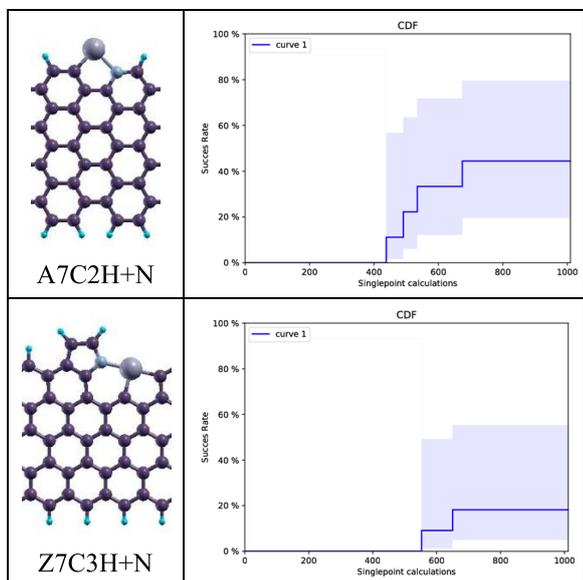


Figure 3. Global minimum and success rate of selected N-doped SAC Pt-G structures.

The results confirm the preferential adsorption of Pt on the graphene edge, where Pt tends to be incorporated within 5- and 6-membered rings. N-doped structures are more difficult to model versus their counterparts, exhibiting lower success rates due

to the increased degree of freedom, but in agreement with prior findings, N tends to adsorb adjacent to Pt [11].

4. Conclusion

The machine learning-based GOFEE algorithm was implemented to perform a structure search on SAC Pt-G systems, including armchair nanoribbons, zigzag nanoribbons, and flake graphene resembling coronene. The results exhibit a high success rate, indicating the successful identification of the global minima across different independent runs and confirm the preferential edge adsorption of Pt, forming 5- and 6-membered rings on the graphene edge.

Further improvements to the GOFEE code may be implemented to optimize the acquisition function for increased accuracy and lower computational cost. Future work on this study includes examining the adsorption of intermediates involved in oxygen reduction and carbon monoxide electrooxidation to assess the catalyst reactivity.

References

- (1) K. Jiang et al., *CCS Chem* **3**, 241 (2021).
- (2) J. Liu et al., *Nat Commun* **8**, 1 (2017).
- (3) J. Liu et al., *Angewandte Chemie International Edition* **58**, 1163 (2019).
- (4) S. Sun et al., *Sci Rep* **3**, 1775 (2013).
- (5) C. Tsounis et al., *Adv Funct Materials* **32**, 2203067 (2022).
- (6) K. Yamazaki et al., *The Journal of Physical Chemistry C* **122**, 27292 (2018).
- (7) S. A. Wella et al., *Nanoscale Adv.* **1**, 1165 (2019).
- (8) S. A. Wella et al., *J. Chem. Phys.* **152**, 104707 (2020).
- (9) M. K. Bisbo and B. Hammer, *Phys. Rev. Lett.* **124**, 086102 (2020).
- (10) M. K. Bisbo and B. Hammer, *Phys. Rev. B* **105**, 245404 (2022).
- (11) R. Sugimoto et al., *J. Phys. Chem. C* **125**, 2900

- (2021).
- (12) J. J. Mortensen et al., Phys. Rev. B **71**, 035109 (2005).
- (13) J. Enkovaara et al., J. Phys.: Condens. Matter **22**, 253202 (2010).
- (14) A. H. Larsen et al., Phys. Rev. B **80**, 195112 (2009).
- (15) J. P. Perdew et al., Phys. Rev. Lett. **77**, 3865 (1996).
- (16) K. F. Garrity et al., Computational Materials Science **81**, 446 (2014).
- (17) P. Giannozzi et al., J. Phys.: Condens. Matter **21**, 395502 (2009).